Journal of Power Sources 243 (2013) 499–507

Contents lists available at SciVerse ScienceDirect

Journal of Power Sources

journal homepage: www.elsevier.com/locate/jpowsour

Activated carbon nanofibers (ACNF) as cathode for single chamber microbial fuel cells (SCMFCs)

Carlo Santoro [a,b,*], Astrid Stadlhofer [c], Viktor Hacker [c,**], Gaetano Squadrito [d], Uwe Schröder [e], Baikun Li [a,b,*]

[a] Department of Civil and Environmental Engineering, University of Connecticut, 261 Glenbrook Road, Unit 3037, 06269 Storrs, CT, USA
[b] Center for Clean Energy Engineering, University of Connecticut, 44 Weaver Road, 06269 Storrs, CT, USA
[c] Department of Chemical Engineering and Environmental Technology, Graz University of Technology, Graz, Austria
[d] Consiglio Nazionale delle Ricerche, Istituto di Tecnologie Avanzate per l'Energia (CNR-ITAE), Via Salita S. Lucia sopra Contesse n. 5, 98126 S. Lucia, Messina, Italy
[e] Technische Universität Braunschweig, Institute of Environmental and Sustainable Chemistry, Hagenring 30, 38106 Braunschweig, Germany

HIGHLIGHTS

- Carbon nanofibers were activated chemically using HNO_3.
- In abiotic conditions, ACNF performed better than CNF but lower than Pt/C.
- In biotic conditions, Pt cathode decreased much faster than ACNF/CNF.
- The presence of H_2S/HS^- and the absence of O_2 were detected in SCMFCs.
- MFC performance in mixed liquor was lower than in synthetic wastewater.

ARTICLE INFO

Article history:
Received 3 May 2013
Received in revised form
10 June 2013
Accepted 11 June 2013
Available online 18 June 2013

Keywords:
Carbon nanofibers (CNF)
Microbial fuel cell (MFC)
Power generation
Linear sweep voltammetry (LSV)
Long terms performances

ABSTRACT

The suitability of carbon nanofibers (CNF) based cathodes as alternative to the platinum (Pt)-based cathode in single chamber microbial fuel cells (SCMFCs) were extensively studied over 3-month operational period. MFCs were fed with two solutions: synthetic wastewater (phosphate buffer (PBS) plus sodium acetate) and real wastewater (mixed liquor suspendedsolid (MLSS) solution). CNFs were chemically activated using HNO_3 and then hot pressed on a carbon cloth support to increase surface area. The cathode polarization showed a better behavior of the clean Pt-based cathode in abiotic conditions. The activation of the nanofibers (ACNFs) gave an advantage to the cathode performances compared to the raw CNFs. The SCMFCs fed with PBS showed four times higher power generation compared to MLSS solution. All the cathodes showed a decrease in performances over time, and the advantage of the Pt over CNF/ACNF disappeared. CNF/ACNF cathodes showed more stability in performances in long time operations. Biofilm formation, salt precipitations on the cathode, and the presence of hydrogen sulfide decreased the activity of Pt cathodes. A degradation and Pt detachment were noticed on Pt cathodes over time. In contrast, CNF/ACNF cathodes exhibited less deterioration throughout the operational period, which demonstrated a great potential as cost-effective cathodes for long-term operation.

1. Introduction

Developing a self-sustainable technology to overcome the shortage of renewable energy and achieve affordable wastewater treatment is a critical challenge. Microbial fuel cell (MFC) technology has a great potential to be an alternative for generating environmentally friendly energy and simultaneously treating wastewater [1,2]. The majority of the studies on MFCs have been conducted in lab scale with the purpose of increasing power generation and decreasing the capital costs [3]. Due to the high activation losses at the cathode [4], a catalyst should be added to increase the oxygen reduction reaction (ORR) kinetic [4]. Particularly, noble metals catalysts (e.g. platinum (Pt)) have been widely used at the cathode, but Pt causes the high cost of the MFC systems,

* Corresponding authors. Department of Civil and Environmental Engineering, University of Connecticut, 261 Glenbrook Road, Unit 3037, 06269 Storrs, CT, USA.
** Corresponding author.
E-mail addresses: carlo.santoro@uconn.edu, ka.santo@hotmail.it (C. Santoro), viktor.hacker@tugraz.at (V. Hacker), baikun@engr.uconn.edu (B. Li).

0378-7753/$ – see front matter © 2013 Elsevier B.V. All rights reserved.
http://dx.doi.org/10.1016/j.jpowsour.2013.06.061

and hinders large-scale MFC design, operation, and commercialization [5,6].

Recently, different metals and non-metal have been studied as the alternative cathodic catalysts to lower the material costs and improve ORR. Metal based cathode (e.g. manganese dioxide [7,8], cobalt (CoTMPP, [9]), pyrolyzed iron(II) phthalocyanine [9] non-PGM [10,11], etc. [5,12]) were developed and compared with the Pt-based cathode. Non-metal cathodes (e.g. activated carbon [13,14] and nitrogen-doped granules [15], carbon powder [16] and nanotubes [17] and carbon nanofibers [18]) exhibited higher ORR activity than Pt-based cathodes. Among these novel cathodic materials, carbon nanofibers (CNFs) are promising, due to high ORR and great surface area. CNFs were examined as novel anodes in MFCs, and demonstrated high biofilm capacity and excellent electron transfer [19]. CNFs were also used in chemical fuel cells as catalysts or catalysts support [20]. The distinct characteristics of the CNFs include (i) great surface area, (ii) excellent chemical stability, (iii) high electrical conductivity, (iv) high mechanical strength, and (v) low cost [20]. Generally, CNFs are treated thermally [21] or chemically [22] in order to remove the metals impurities (e.g. iron, sulfur, etc.) from the fibers, increase the surface area, and increase the ORR [22].

Even though many studies have been conducted to develop novel metal-based and non-metal-based cathodes in MFCs, CNFs have not been thoroughly studied as novel cathode. The objective of this study is to extensively investigate the potential of CNFs as low-cost cathode with high electrocatalytic activity in MFCs treating wastewater. There are four tasks in this study. First, two types of CNFs (raw CNF and chemically activated CNF) were compared in MFCs, and the effects of chemical activation on CNF performance were illuminated. Second, the effects of CNF loadings and hydrophobic coating contents (Polytetrafluoroethylene, PTFE) on cathode performances were determined using electrochemical characterization (e.g. single electrode polarizations, open circuit potentials (OCP)). Third, the CNF-based and Pt-based cathodes were compared side-by-side in single chamber MFCs (SCMFCs) fed with two types of solutions (synthetic wastewater and mixed liquor suspended solids) over an operational period of 3 months. Finally, power curves were recorded over the experimental period for all types of cathodes to determine the fundamental advantage of CNFs over Pt as cost-effective cathodes in MFCs.

2. Materials and method

2.1. Cathode preparation

2.1.1. Chemical activation of CNFs

Tubular CNFs (HRF150FF-LHT, Electrovac) were used as raw CNFs. For chemical activation of CNFs, the tubular CNFs with an average outer diameter (OD) of 150 nm were oxidized in nitric acid (≥69 wt%) under a reflux at 118 °C for 5 h. After cooling down to room temperature, the CNF material was washed with deionized water until the filtrate was neutral and then dried at 80 °C.

2.1.2. The CNF cathode preparation

The CNF cathodes were prepared using a sedimentation method as showed previously [23,24]. The pretreated CNFs and PTFE (Dyneon TF 5035 PTFE dispersion) were dispersed in deionized water and sonicated for 30 min. This dispersion mixture was then deposited on a carbon cloth (30% wt PTFE treated, Fuel Cell Earth), which was fixed on a round glass frit with vacuum. The raw CNFs (label as CNF) and chemically activated CNFs (label as ACNF) were compared at different carbon loadings and PTFE contents (Table 1). Two types of CNFs had different PTFE contents: CNF 1 with 33% wt PTFE and the CNF loading 14 mg cm^{-2} and CNF2 with 20% wt PTFE and 12 mg cm^{-2}. Three types of ACNFs had different types of PTFE contents: ACNF1 with 20% wt PTFE and high ACNF loading of 11 mg cm^{-2}, ACNF3 with 14% PTFE and ACNF loading of 8 mg cm^{-2}, and ACNF3 with 14% PTFE and low ACNF loading of 5 mg cm^{-2}. After sedimentation on the carbon cloth, the cathodes were hot-pressed at 280 °C and 12 kN for 20 min. The CNF and ACNF were compared with Pt-based cathode with a catalyst loading of 0.5 mg Pt cm^{-2} prepared as previously described [25].

2.2. Cathode material characterization

2.2.1. Surface area analysis

Specific surface areas were calculated through the application of the BET model [26] using the adsorption isotherms. An ASAP 2020 Physisorption Analyzer (Micromeritics Instrument Corporation) was used to measure the BET. The CNF cathodes were first degassed at 300 °C for 12 h and then analyzed for nitrogen sorption at 77 K.

2.2.2. SEM observation of CNF cathodes

The structure of the active layer on the CNF/ACNF cathodes was observed by a field emission scanning electron microscope (FEI, XL30-SFEG). Duplicate samples of 10 × 10 mm^2 were cut from fresh cathodes, and then mounted on the sample holder by bi-adhesive conducting film. Due to the conductive nature of the cathode samples, no additional treatment was applied. Before the observation, the samples were maintained under vacuum inside the SEM observation chamber for 2 h.

2.3. SCMFC configuration and operation

The CNF/ACNF cathodes and Pt cathodes were installed individually in single chamber microbial fuel cells (SCMFCs). Each type of cathodes with the geometric area of 1 cm^2 was tested in duplicate. The volume of SCMFC was 130 ml. Untreated carbon cloth (Fuel Cell Earth) with a geometric area of 20 cm^2 was used as the anode electrodes as previously described [27]. It was found previously that the anode geometric area of 20 cm^2 was not the limiting factor for the MFCs performances [28]. The anode and cathode were connected through an external resistance (R_{ext}) of 1197 Ω throughout the experimental period (Fig. 1a). The voltage (V) was recorded with a frequency of 2 h using a Keithley 2700 data logging system. The current ($I = V/R$) and the power ($P = V \times I$) generation were calculated based on the Ohm's law. Current density and power density were referred to the cathode geometric area (1 cm^2).

The SCMFCs were operated in batch mode for 3 months. The anodes were well colonized by electrogenic bacteria for at least 6 months before being used in SCMFCs. The SCMFCs were inoculated with raw wastewater (taken from the University of Connecticut Wastewater treatment plant) and sodium acetate (NaOAc). Two anodic solutions were tested in SCMFCs: i) Synthetic wastewater consisting of phosphate buffer solution (PBS) and 3 g L^{-1} sodium acetate (NaOAc); ii) Mixed liquor suspended solid (MLSS) solution taking from aeration tanks. MLSS solution was selected due to high amounts of soluble chemical oxygen demand (sCOD),

Table 1
The cathode specification and nomenclature for raw CNFs and activated CNFs.

	PTFE (w%)	CNF (mg cm^{-2})	Abbreviation
CN	33	14	CNF1
CN	20	12	CNF2
CN activ.	20	11	ACNF1
CN activ.	14	8	ACNF2
CN activ.	14	5	ACNF3
Cloth + MPL + 0.5 mg Pt cm^{-2}			Pt

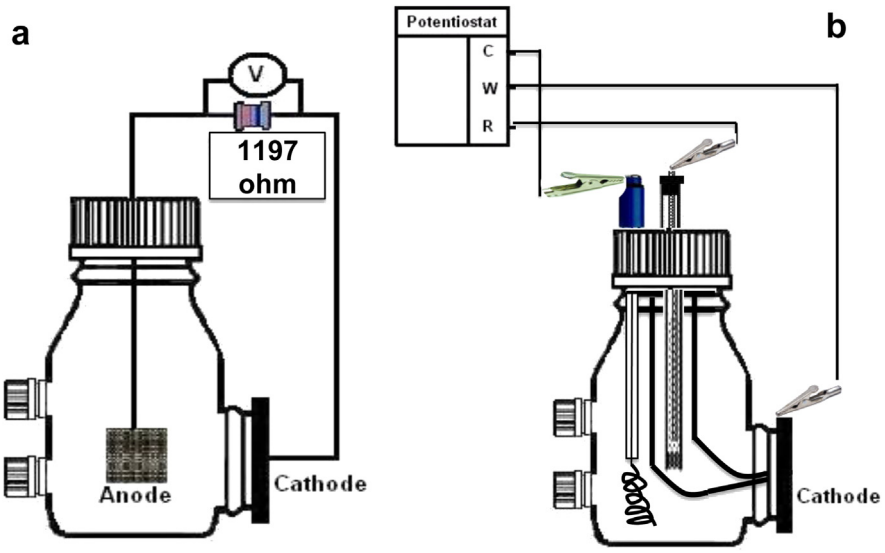

Fig. 1. The SCMFC setup (a) and the cathode LSV measurement setup (b).

high amounts of microorganisms, and higher solution conductivity compared to raw wastewater.

For the SCMFCs fed with PBS solution, the anodic solution was completely refreshed after 21, 42, and 63 days, and NaOAc (2 g L^{-1}) was added on a weekly base. Due to the slight water evaporation through the air-cathodes in SCMFCs, raw wastewater was added to fill the anodic chamber. For the SCMFCs fed with MLSS solution, the anodic solution was refreshed on a weekly base. The PBS solution had an initial pH of 7.2–7.3 and solution conductivity of 8.4–8.6 mS cm^{-1}, and the MLSS solution had an initial pH of 7.6–7.8 and a solution conductivity of 1.35–1.46 mS cm^{-1}, and an initial sCOD concentration of 0.65–0.71 g L^{-1}. Our previous study showed a COD removal efficiency of 50% in SCMFCs with cathode area of 1 cm^2 [28].

2.4. Electrochemical measurements of SCMFCs

Electrochemical cathode polarization curves (linear sweep voltammetry (LSV)) were measured in a three-electrode configuration for all cathodes tested. A platinum wire was used as counter electrode, an Ag/AgCl electrode as reference, and the cathode to be tested was used as the working electrode (Fig. 1b). A modified Luggin capillary was used to decrease the ohmic losses between the counter and the working electrode. The LSV curves were performed at low scan rate (0.2 mV s^{-1}) using a potentiostat (Gamry P600). Preliminary tests were conducted by purging nitrogen (over night) and purging air (DO > 5 mg DO L^{-1}) in PBS solution. Cathode Open Circuit Potentials (OCP) were measured using a voltmeter connecting the two channels (the cathode and the reference electrode (Ag/AgCl: +197 mV vs standard hydrogen electrode, SHE)) after anode and cathode were disconnected for at least 1 h. The LSV tests with the anodic solution were performed after the SCMFCs were in OCP measurement for 3 h.

2.5. The measurement of O_2 and H_2S/HS^- in anodic solution

In SCMFCs, the air-cathode directly contacted the anodic solution, thus oxygen might penetrate through air-cathode into the anode chamber and have harmful impacts on anaerobic electrogenic microorganisms. Thereby, it is critical to maintain the anaerobic condition in anode chamber in order to achieve high performance of SCMFCs. In this study, Cyclic Voltammetry (CV) using gold/mercury (Au/Hg) microelectrodes [29] were performed to verify the absence of oxygen and the presence of hydrogen sulphide in the anodic chamber close to the air-cathode. Platinum (Pt) wire was used as the counter electrode and Silver/Silver Chloride (Ag/AgCl) was used as the reference electrode. The electrode reactions at the Au/Hg microelectrode were previously reported [29]. Particularly, there will be a peak in the CV curve at $E_0 = -0.29$ V (vs Ag/AgCl), if oxygen is present (with the formation of H_2O_2 ($E_0 = -1.19$ V (vs Ag/AgCl)). The presence of hydrogen sulfide (H_2S/HS^-) caused by anaerobic reduction reactions can be detected with a peak at −0.75 V vs Ag/AgCl [29]. The absence of oxygen and the presence of hydrogen sulphide indicate the strict anaerobic condition. The CV was performed at a high scan rate (3 V s^{-1}) in the range −2/-0.1 V. The measurements were conducted in the SCMFCs at day 1, 57 and 78. During the measurement, the Au/Hg microelectrode was inserted to the location of anode chamber adjacent to the cathode, and moved close to the cathode. The peaks of oxygen and hydrogen sulphide were measured.

3. Results and discussion

3.1. CNF/ACNF cathode material characterization

The cathodes SEM images showed the fiber sections for CNFs and ACNFs (Fig. 2a and b), and the diameter of the fibers ranged between 50 and 200 nm. On the other hand, the surface of the Pt-based cathode was smooth and flat (Fig. 2c). The good connection among the CNFs and ACNFs fibers was expected to enhance electron transfer compared with Pt-surface. Moreover, some fibers were completely empty (nanotubes), while other fibers were completely perforated and transparent when high electron beam was used (Fig. 2d). The roughness of the ACNFs was captured by the SEM images (Fig. 2d). The chemical activation led to an increase in the surface area especially in the nanometer range (Fig. 2e), which is important to enhance the ORR as previously showed [22]. The comparison of the surface properties of raw CNFs and ACNFs showed that the activation treatment of CNFs increased the specific surface area, with a specific surface area (BET) of CNF being 143 and of ACNFs being 175 g m^{-2}. In this regard, the chemical activation effectively obtained carbons with high surface area and increased the micropore size distribution [22]. The BET analysis showed a higher pore volume in correspondence of smaller average pore size (Fig. 2e). Moreover, the chemical acidic treatment with HNO_3

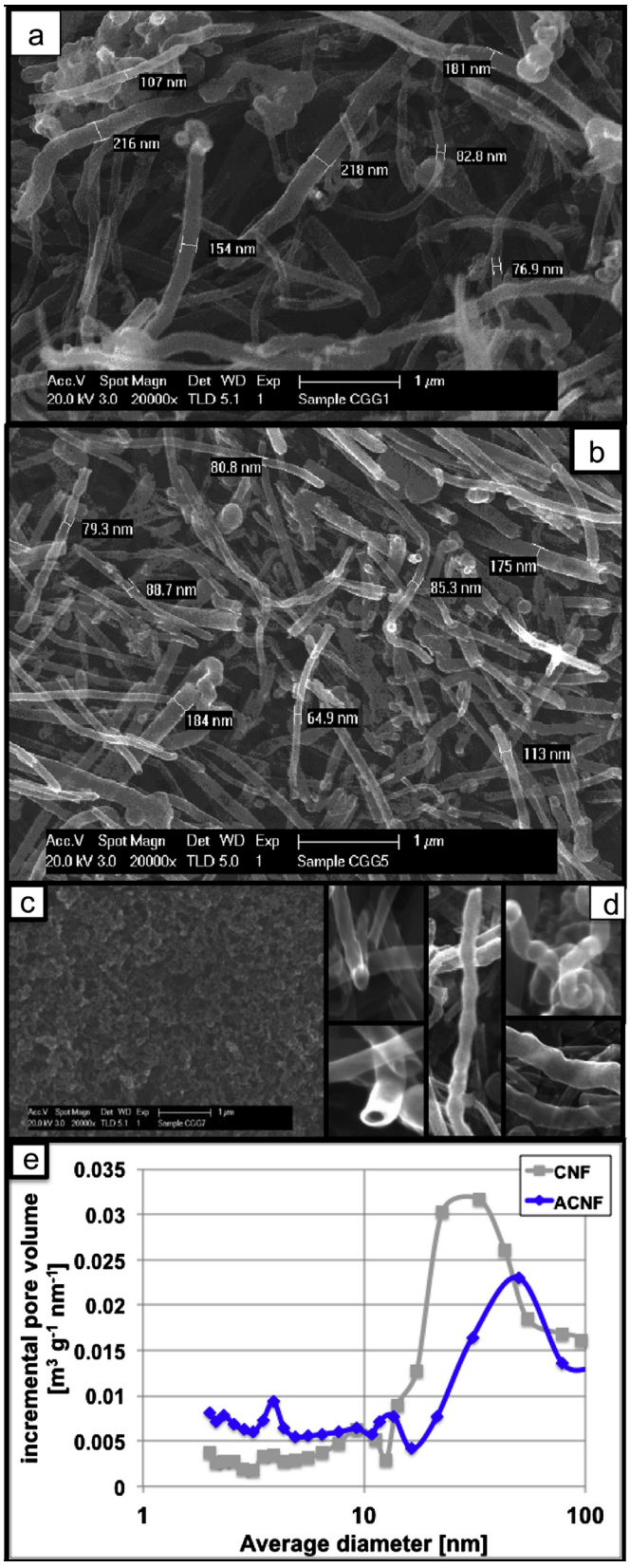

Fig. 2. The SEM images of the CNF (a), ACNF (b) and Pt-based cathode (c) with the same resolution. The SEM images show the transparency and roughness of the ACNFs (d). Pore size distribution of the CNF (gray) and ACNF (blue) cathode (e). (For interpretation of the references to color in this figure legend, the reader is referred to the web version of this article.)

increased the presence of functional groups (i.g. nitrogen and oxygen [15,16]) on the carbon surfaces. Those functional groups could also be also responsible for the increase in electrocatalytic activity of the oxygen reduction reaction (ORR) [15].

3.2. Electrochemical characterization of clean cathodes

The electrochemical characterization of clean cathodes was conducted in linear sweep voltammetry (LSV) before the 3-month SCMFC operation. Nitrogen (Fig. 3a) and air (Fig. 3b) were purged into the abiotic PBS solution in order to obtain an initial characterization (ORR polarization curve) of clean cathodes. A low catalytic activity was observed in all cathodes when nitrogen was purged, indicting the lack of oxygen for ORR (Fig. 3a). Catalytic activities of all cathodes substantially increased when air was purged, among which Pt-based cathode showed the best electrocatalytic activity (Fig. 3b). ACNFs had lower cathode polarization curve than Pt, but higher than the raw CNFs, which well demonstrated the advantage of chemical activation of CNFs for electrochemical oxygen reduction. The activation of the carbon nanofibers enhanced the catalytic activity in the reduction of oxygen.

There was no clear difference between two types of raw CNF cathodes (CNF1 and CNF2), even though they had different hydrophobic agent contents (33% wt vs 20% wt PTFE). A slight difference among three types of ACNFs was detected in the cathode LSVs curves. Particularly, ACNF3 with the lowest CNF loading (5 mg cm^{-2}) had a lower catalytic activity than ACNF1 and ACNF2. In fact, the surface of ACNF3 was not homogenous due to the low CNF loading. No significant difference was detected between ACNF1 and ACNF2, even though ACNF1 had higher PTFE content (20% wt) and higher CNF loading than ACNF2. An increase in CNF loading led to a progressive increase in performance, which was in agreement with previous studies [18]. The chemical activation led to an increase in the available surface area (Fig. 2e) and enhanced the oxygen reduction reaction. Moreover, previous studies using XPS technique found that the chemical activation with HNO_3 led to the binding of nitrogen and oxygen functional groups [15], and the nitrogen functional groups on the surface increased during the activation of graphite granules with nitric acid [15], thus enhancing the ORR. Similar superficial nitrogen groups were found after the chemical treatment of the carbon powder with nitric acid [16], and the enhancement of carbon performance after the chemical activation was attributed to the increase in surface area and nitrogen functional groups [15,16]. The results from this study showed that proper amounts of PTFE contents (>20% wt) and CNF loadings (>8 mg cm^{-2}) could maintain the good performances of CNFs/ACNFs, further increase in PTFE contents and CNF loadings might not necessarily increase the performance.

3.3. The cathode performance in the SCMFCs over 3-month

3.3.1. Open circuit potentials (OCP) of cathodes

Based on the LSV results of the freshly prepared cathodes (Fig. 3), CNF 2 and ACNF2 exhibited the best performance in each category of cathode materials, and their performance were the optimum in terms of the cost of materials (PTFE content and CNF loadings). Thereby, they were tested later in SCMFCs over the 3-month operational period. The cathode OCP results showed that on Day 0, Pt cathode had the highest OCP (0.43 V), followed by ACNF (0.3–0.32 V), and the CNF had the lowest OCP (0.22–0.23 V) (Fig. 4). These cathode OCP values were much lower values compared to the theoretical values (the ORR is 1.229 V (vs SHE) at pH = 0). In this study, the pH of the SCMFC solution was neutral (pH = 7), and the theoretical potential was 0.82 V (vs SHE). The

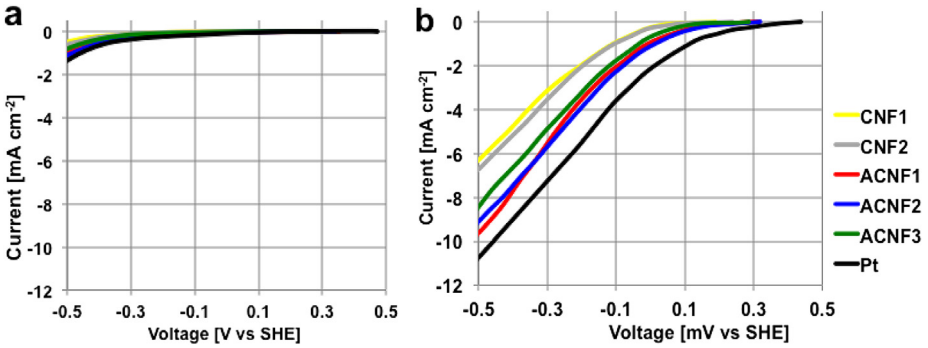

Fig. 3. The polarization curves of cathodes in PBS solution purging nitrogen (a) and purging air (b).

reason of the low cathode OCP values might be caused by the configuration of the air-cathode SCMFCs, in which the cathode is directly in contact with the solution that may cause cathode flooding and increase the activation losses. This was previously identified as the most significant limitation in the cathode activity [30]. All cathode OCPs steadily decreased over the operational period (Fig. 4). The anodic potential (−0.287 V and −0.323 V (vs SHE)) remained close to the theoretical value (−0.296 vs SHE) over the entire experimentation period, regardless of the types of cathode used (data not shown).

The anodic solutions in SCMFCs affected the cathode OCP during the operational period. For the SCMFCs fed with PBS solution and NaOAc, the Pt-based cathode OCP decreased from the initial (day 0) values of 420–435 mV to 293–302 mV on day 8, and dropped to 252–265 mV on day 29, to 219–231 mV on day 57, and finally to 202–214 mV on day 78 (Fig. 4a). The OCP of ACNFs decreased to 146–167 mV on day 78, and the OCPs of CNF were the lowest. For the SCMFCs fed with MLSS solution, the Pt-based cathode OCP was 109–122 mV, the ACNF2 OCPs were 43–55 mV, and CNF2 OCPs were 22–30 mV on day 78 (Fig. 4b), which were much lower than those fed with PBS solution and NaOAc.

3.3.2. Oxygen and hydrogen sulfide measurements in the anodic solution

Throughout the operational period, the anodic chamber was maintained in anaerobic conditions. In fact, the oxygen initially contained in anodic solution was consumed by microorganisms. The oxygen needed for the cathodic ORR was diffused from the outside atmosphere. The CVs measured using a microelectrode confirmed the complete absence of oxygen in the anodic chamber independently from the cathodes used (Fig. 5). Additional measurements conducted with an oxygen probe inserted into the anodic chamber also showed dissolved oxygen (DO) equal to 0.05 mg DO L^{-1} (equal to the accuracy of the instrument), which indicated the anaerobic condition of anode chambers in SCMFCs. Moreover, the anodic OCP remained in the negative range close to the theoretical value of acetate oxidation (−0.287 V and −0.323 V (vs SHE), confirming the strict anaerobic conditions along the operational period. Previous studies with anodic chamber filled with wastewater and sodium acetate [31] or urine [32] showed no oxygen detection in proximity of the cathode along the experimentation period. A clear peak of H_2S/HS^- instead was visible in both anodic solutions investigated. The H_2S/HS^- was probably the product of the microbial activity of the sulfur reducing bacteria that were able to transform the SO_4 ions into H_2S/HS^-[33]. The wastewater added weekly on the SCMFCs fed with PBS had a sulfate initial concentration of 11–15 mg L^{-1} (Fig. 5a), while in the MLSS solution, the initial concentration was much higher (45–68 mg L^{-1}) (Fig. 5b). Particularly, in the case of PBS anodic solution, the peak of H_2S/HS^- was almost negligible but then it increased over time at day 57 and 78 (Fig. 5a). Due to the much higher sulfate concentration in the MLSS, the peak at 0.75 V was 5–7 times higher than in the SCMFCs with anodic chamber fed with PBS (Fig. 5b).

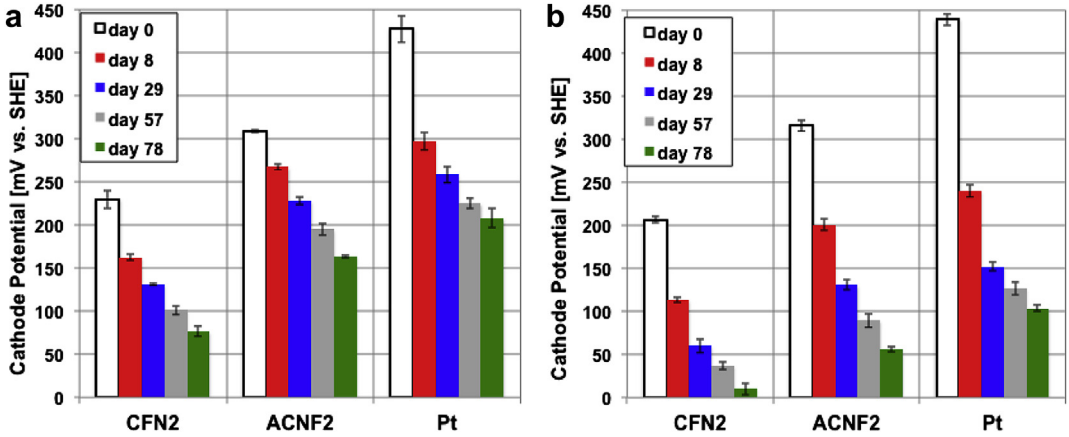

Fig. 4. The cathode OCP in SCMFCs fed with PBS + NaOAc (a) and MLSS (b) over the 3-month operational period. Day 0 (white), 8 (red), 29 (blue), 57 (gray) and 78 (green). (For interpretation of the references to color in this figure legend, the reader is referred to the web version of this article.)

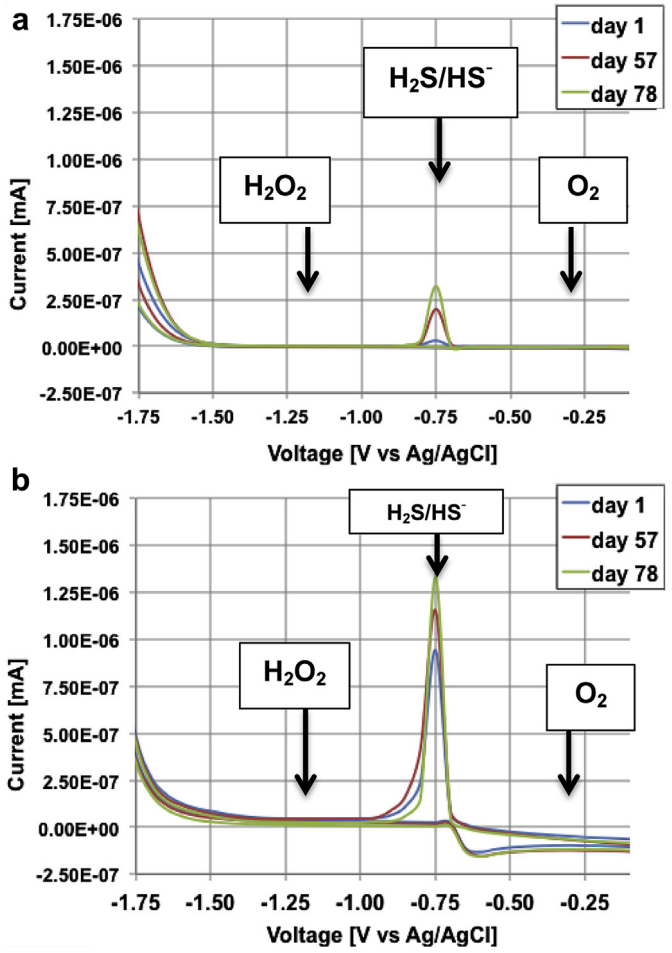

Fig. 5. Cyclic voltammograms (CV) showing presence of oxygen (−0.25 V), hydrogen sulfide (−0.75 V) and hydrogen peroxide (−1.23 V) in the SCMFCs with PBS (a) and MLSS (b) in the anodic chamber.

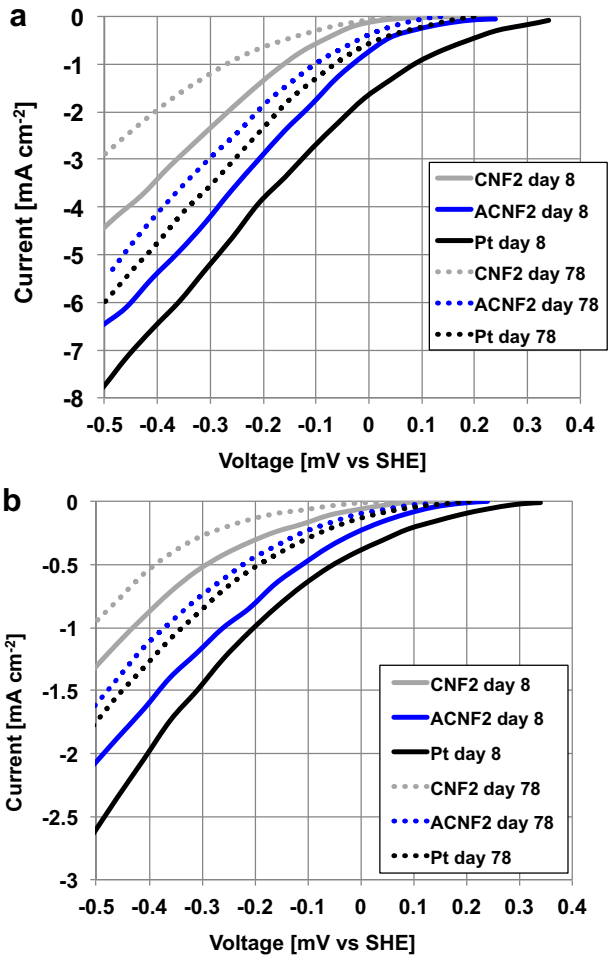

Fig. 6. The cathode polarization curves (CNF2, ACNF2 and Pt) in SCMFCs fed with PBS and NaOAc (day 8 and day 78 (a)) and with activated sludge (day 8 and day 78 (b)). (Note: day 8 curves are identified with solid lines and day 78 curves are identified with dashed lines).

3.3.3. The electrochemical characterization of cathodes over 3-month

The polarization curves of CNF/ACNF cathodes were compared with Pt-cathode over the operational period (Day 8 and Day 78, Fig. 6). The cathode LSVs clearly showed the decrease in electrocatalytic activity over time compared to the initial LSVs. The direct contact of the cathode with the anodic solution led to the complete oxygen consumption on the cathode surface, which was enhanced by the presence of microorganisms in the electrolyte and confirmed by the CV curves with no peaks of O_2 (Fig. 5). On Day 8, the differences among cathodes (CNF/ACNF and Pt) were clearly visible (Fig. 6). Pt-based cathode reached the highest, ACNF2 second, and CNF2 the lowest current density. In addition, the cathode LSVs in PBS solution (Fig. 6a) had much higher catalytic activity than in MLSS solution (Fig. 6b), which might be caused by the higher solution conductivity (8.4–8.6 mS cm^{-1} vs 1.35–1.46 mS cm^{-1}). The effect of solution conductivity on the cathode performance was reported previously [34].

The catalytic activity of all cathodes deteriorated over time and the cathode polarization curves showed a decrease in the OCP values (initial point with no current) (Fig. 6). The advantage of Pt over CNF/ACNF substantially reduced over time. Particularly the gap between the Pt-based and ACNF2 became smaller on day 78 in the PBS solution (Fig. 6a) and almost disappeared in the MLSS solution (Fig. 6b). Much higher amounts of microorganisms and pollutants in the MLSS solution than in the PBS solution inhibited the Pt catalytic activity in a faster way. Biofilm formation and salt precipitations on the cathodes were responsible for the decline of the performances in mediator-less MFCs [6]. In fact, thicker biofilms growing over time increased the mass transport resistance of the protons moving from the anodic solution to the catalytic sites [6]. A recent study observed the precipitation of salts and the penetration of salt through the cathode structure [31], which deteriorated the MFC performances due to the pore clogging and the consequent decrease in oxygen transport from the atmosphere to the catalytic sites.

The activities of CNF/ACNF and Pt cathodes were affected at different levels with the presence of sulfate/sulfide in anodic chambers. The behavior of sulfate/sulfide redox couple using the Pourbaix diagram was described previously [35]. Due to the neutral/slightly alkaline pH (pH 7–8) of the anodic solutions in this study, the hydrogen sulfide was in both forms H_2S and HS^- since the acid dissociation constant was at 7.2. The CV curves using the Au/Hg microelectrode showed a high peak of H_2S/HS^- (Fig. 5), which was generally associated with the loss in catalytic activity of Pt [30,36–38]. Several studies showed the severe Pt poisoning due to the presence of sulfur compounds (mainly hydrogen sulfide and sulfur dioxide) even at low concentrations (ppm) [36–38]. In contrary, the ACNF/CNF cathodes were not affected by the presence

of sulfide, since their activities were mainly attributed to the fibers characteristics, and the fiber activation created a greater number of pores with nanometric size (confirmed by the BET, Fig. 2e) that increased the numbers of catalytic centers and consequently enhanced the cathode performances.

Biofilms formed on all cathode surfaces tested (Fig. 7), regardless of the cathode composition. Previous studies found the biofilm formation on cathodes increased the proton mass transfer resistance and limited the performances in mediator-less MFCs over time. At the end of 3-month period, thick and well-developed biofilms were visible at naked eyes (Fig. 7) with dissimilarities among different cathodes. In the case of Pt-based cathodes, biofilms contained the black particles identified as carbon/Pt (C/Pt) particles, which were used to fabricate the cathode (Fig. 7a). It is possible that the microorganisms sticking on the catalyst surface were able to remove the C/Pt particles from the carbon cloth and the Pt catalytic activity was severely compromised over time. In contrast, the biofilms formed on the CNF/ACNF cathodes did not have any black particles, implying that biofilms would not erode the cathode surface over time (Fig. 7b). This difference could be caused by the preparation methods for the Pt-based and CNF/ACNF cathodes. For the Pt cathodes, the Pt-based layer was added by brushing the C/Pt mixture on the carbon cloth [25] and the mixture was dried at air temperature, while for the CNF/ACNF cathodes, the raw/activated CNF mixture was hot pressed on the carbon cloth, and thus exhibiting less material deterioration over time and optimal for long-term MFC operation.

3.3.4. *The voltage trends and power generation of SCMFCs over 3-month period*

The SCMFCs fed with PBS solution (synthetic wastewater) and MLSS were operated in batch mode for 3 months (12 weeks). The SCMFCs fed with synthetic wastewater (PBS + NaOAc) had much higher voltage outputs (Fig. 8a) than those fed with the MLSS solution (Fig. 8b), which was caused by the difference in solution conductivity and substrate used. The PBS solution had much higher solution conductivity than MLSS solution (8.4–8.6 mS cm^{-1} vs. 1.3–1.46 mS cm^{-1}), which reduced the ohmic resistance of the solution and enhanced the voltage outputs. Easily degradable organic compounds (NaOAc) in the synthetic wastewater and the more complex organic compounds (e.g. in MLSS) also affected the SCMFC performances.

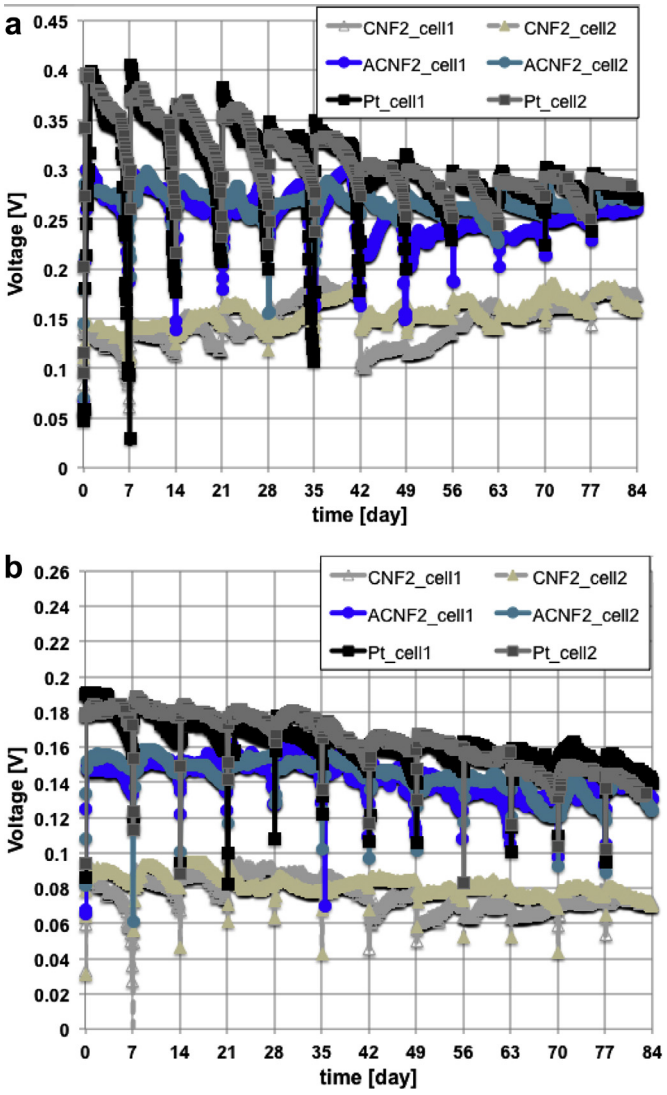

Fig. 8. The voltage of the SCMFCs with CNF2, ACNF2 and Pt-based cathodes fed with in PBS solution (a) and MLSS solution (b).

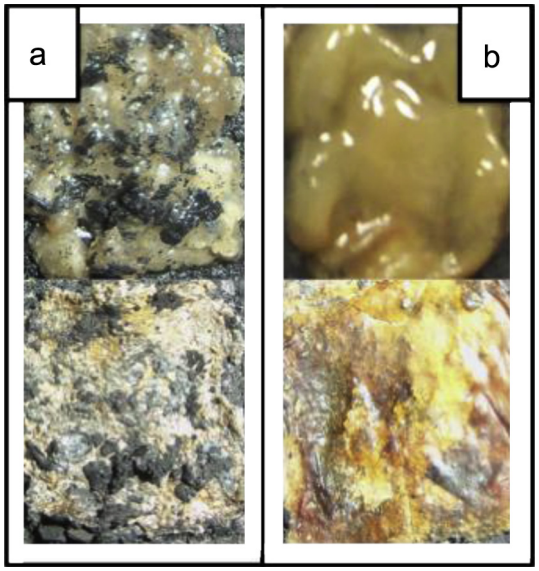

Fig. 7. Biofilm formation (wet and dry) at the end of the experimentation observed on the Pt-based (a) and ACNF2 (b) cathodes facing the anodic solution.

The voltage outputs of SCMFCs with CNF2, ACNF2, and Pt cathodes over 3 months showed the similar patterns as the cathode polarizations curves (Fig. 6), with Pt the highest, ACNF2 second, and CNF 2 the lowest (Fig. 8a). Two major findings should be noted. First, the advantage of Pt over CNF2 and ACNF2 steadily decreased over time. Second, the voltage outputs of CNF2 and ACNF2 cathodes were much more stable than Pt cathodes, and remain almost same throughout the 3-month operational period. This was caused by the structure difference between CNF/ACNF and Pt cathodes as discussed in previous session (3.3.3). In addition, the CNFs activated with HNO_3 were not affected by the presence of sulfide species, while the Pt lost substantially the catalytic activity of ORR.

The power generation followed the voltage trend and the cathode polarization behavior over time. The initial power generation (day 1) achieved by the Pt-based cathode was the highest among cathodes tested (Fig. 9), but the power output of Pt cathodes steadily decreased over time, while CNF/ACNF cathodes exhibited stable power output. The peaks of power generation of the SCMFCs with PBS solution and NaOAc were the following: 1044–

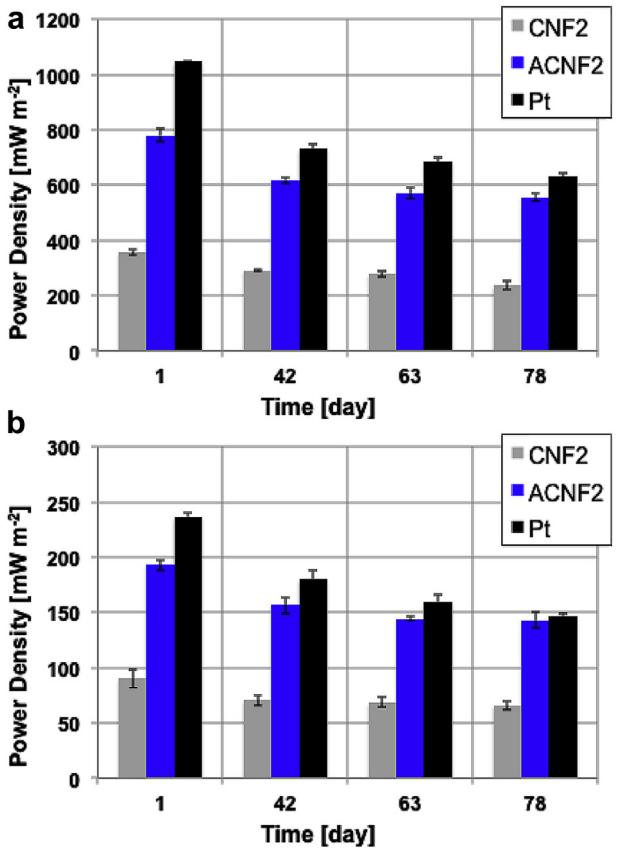

Fig. 9. The peak of power curves in SCMFCs fed with PBS solution (a) and MLSS (b) over 3-month period.

1052 mW m^{-2} (Pt-based), 756–803 mW m^{-2} (ACNF2), and 345–370 mW m^{-2} (CN2) (Fig. 9a). After 11 weeks (day 78), the peak of power generation in the Pt-based SCMFCs fed with PBS solution reduced 40–45%, while reduced only 25–30% in the CNF/ACNF. In the case of MLSS solution, the peaks of power generation were lower than those in PBS solution: 233–245 mW m^{-2} (Pt-based), 185–199 mW m^{-2} (ACNF2) and 87–100 mW m^{-2} (CN2) (Fig. 9b). After 78 days, the peak of power generation of Pt-based cathode was similar to the ACNF cathode (143–147 mW m^{-2}).

There were two main factors leading to the higher power generation of ACNF2 than CNF2. First, the increase in CNF/ACNF surface areas (roughly 20%) especially in the nanometric range enhanced the numbers of catalytic centers and increased the ORR. Second, the addition of nitrogen functional groups on the ACNFC surfaces due to the chemical activation with nitric acid. Those nitrogen functional groups responsible for boosting the cathode reactions were not specifically identified in this study but previously reported [15,16].

The 3-month tests clearly indicated the higher stability of CNF/ACNF cathodes than the Pt-based cathodes (Figs. 6–8). The pollutants in MLSS solution caused the substantial decrease in catalytic activity for the Pt-based cathode (Fig. 9b). In this study, the pollutants were introduced into the SCMFCs by adding wastewater in order to refill the water losses due to evaporation. The pollutants were confirmed by the higher peaks of H_2S/HS^- in the MLSS solutions than in the PBS solution (Fig. 5). In contrast, only a slight decrease in voltage and power generation was noticed for the CNF/ACNF cathodes, probably because those cathodes were not deteriorated by chemical poisoning, and CNF/ACNF did not suffer of fiber detachment with biofilm growth (Fig. 7), and demonstrated a high reliability in long term operation.

3.4. Significance and future application of CNFs and ACNFs as novel cathodes in MFCs

This study extensively investigated the CNF/ACNF as low cost and novel cathode in SCNFCs. Clean Pt-based cathode exhibited high catalytic activity in electrochemical tests when there was no poisoning compound in solutions. The chemical activated ACNF cathodes showed slight lower catalytic activity than Pt cathodes, but much higher performances than the raw CNF cathodes. When exposed to real wastewater containing diverse pollutants, the catalyst poisoning made the Pt activity decreased significantly over time, while there was no particular impact on CNF/ACNF. Consequently, a significant drop in Pt-based SCMFCs over time was underlined, while a stable performance was maintained in the ACNF cathode SCMFCs. The decrease in Pt performances was probably caused by the biofilm growth, the precipitation of compounds on the cathodes and the presence of hydrogen sulfide. The SCMFCs with ACNF cathode had similar performance as those with Pt cathode in long-term operation, which showed a great promise for reducing the capital costs.

Currently, the power generation in MFCs is still low, even though MFCs show the ability to harvest the electricity from the conversion of wastes [39–41]. This study demonstrated a critical aspect associated with MFC performance in different anodic solutions. The SCMFCs fed with PBS solution and easily degradable organics (in relatively high concentration) which were commonly used in many MFC studies, had power generation 4 times as those fed with MLSS solution. The results clearly showed the poisoning effects of the real MLSS solution on Pt cathodes, rather than CNF/ACNF cathodes. This reveals a great potential for CNF/ACNF for treating real wastewater.

4. Conclusions

The CNF/ACNF cathodes were compared with Pt-cathodes in SCMFCs fed with synthetic wastewater (PBS solution + NaOAc) and real wastewater (MLSS solution) over a period of 3-month. Four major conclusions were drawn in this study.

First, the chemical activation of the CNF with HNO_3 (termed as ACNF) increased the specific surface area in the small nanometric size (0.1–5 nm). The nitrogen functional groups bonded on the nanofiber surfaces possibly contributed to the enchantment of the ACNF. In the abiotic electrochemical tests, Pt-based clean cathode showed the best performances, ACNF second, and CNF lowest.

Second, CNF/ACNF cathode SCMFCs showed a higher stability in voltage output and power generation over time than Pt-based cathode SCMFCs. The Pt was poisoned by pollutants (measured as hydrogen sulfide using microelectrodes) in the anodic chamber. Pt-based cathode deteriorated faster and catalyst detachment was observed.

Third, ACNF cathodes could be a reliable cost-effective alternative to Pt-based cathode in SCMFC for long-term operation. The high surface area of ACNFs resulted in a good performance and the hot pressing of ACNFC preparation led to slow deterioration over time.

Fourth, the SCMFCs fed with synthetic wastewater (PBS and NaOAc) showed more than 4 times higher power generation than those fed with MLSS solution. CNF/ACNF cathodes had higher stability than Pt cathodes when treating the real MLSS solution.

Acknowledgment

The project is funded by Office of Naval Research (ONR) Microbial Fuel Cell Program.

References

[1] A. Rinaldi, B. Mecheri, V. Garavaglia, S. Licoccia, P. Di Nardo, E. Traversa, Energy Environ. Sci. 1 (2008) 417–429.
[2] Z. Du, H. Li, T. Gu, Biotechnol. Adv. 25 (2007) 464–482.
[3] J. Wei, P. Liang, X. Huang, Biores. Technol. 102 (2011) 9335–9344.
[4] H. Rismani-Yazdi, S.M. Carver, A.D. Christy, O.H. Tuovinen, J. Power Sources 180 (2008) 683.
[5] E. Martina, B. Tartakovsky, O. Savadogo, Electrochim. Acta 58 (2011) 58–66.
[6] C. Santoro, A. Agrios, U. Pasaogullari, B. Li, Int. J. Hydrogen Energy 36 (2011) 13096–13104.
[7] X. Li, B. Hu, S. Suib, Y. Lei, B. Li, J. Power Sources 195 (2010) 2586–2591.
[8] X. Li, B. Hu, S. Suib, Y. Lei, B. Li, Biochem. Eng. J. 54 (2011) 10–15.
[9] F. Zhao, F. Harnisch, U. Schröder, F. Scholz, P. Bogdanoff, I. Herrmann, Electrochem. Commun. 7 (2005) 1405–1410.
[10] A. Serov, M.H. Robson, M. Smolnik, P. Atanassov, Electrochim. Acta 80 (2012) 213–218.
[11] S. Brocato, A. Serov, P. Atanassov, Electrochim. Acta 87 (2013) 361–365.
[12] A. Ishihara, Y. Ohgi, K. Matsuzawa, S. Mitsushima, K. Ota, Electrochim. Acta 55 (2010) 8005–8012.
[13] H. Dong, H. Yu, X. Wang, Q. Zhou, J. Feng, Water Res. 46 (2012) 5777–5787.
[14] D. Pant, G. Van Bogaert, M. De Smet, L. Diels, K. Vanbroekhoven. Electrochim. Acta. 55(26) 7710–7716.
[15] B. Erable, N. Duteanu, S.M.S. Kumar, Y. Feng, M.M. Ghangrekar, K. Scott, Electrochem. Commun. 11 (2009) 1547–1549.
[16] X. Shi, Y. Feng, X. Wang, H. Lee, J. Liu, Y. Qu, W. He, S.M.S. Kumar, N. Ren, Biores. Tech. 108 (2012) 89–93.
[17] L. Feng, Y. Yan, Y. Chen, L. Wang, Energy Environ. Sci. 4 (2011) 1892–1899.
[18] S. Chen, Y. Chen, G. Hea, S. He, U. Schroder, H. Hou, Biosens. Bioelectron. 34 (2012) 282–285.
[19] U. Karra, S.S. Manickam, J.R. McCutcheon, N. Patel, B. Li, Int. J. Hydrogen Energy 38 (2013) 1588–1597.
[20] B. Sljukic, C.E. Banks, R.G. Compton, J. Iran. Chem. Soc. 2 (2005) 1–25.
[21] M.L. Toebes, J.M.P. van Heeswijk, J.H. Bitter, A.J. van Dillen, K.P. de Jong, Carbon 42 (2004) 307–315.
[22] J.-S. Zheng, X.-S. Zhang, P. Li, X.-G. Zhou, D. Chen, Y. Liu, W.-K. Yuan, Electrochim. Acta 53 (2008) 3587–3596.
[23] V. Hacker, E. Wallnofer, W. Baumgartner, T. Schaffer, J.O. Besenhard, H. Schrottner, M. Schmied, Electrochem. Commun. 7 (2005) 377–382.
[24] E. Wallnöfer, M. Perchthaler, V. Hacker, G. Squadrito, J. Power Sources 188 (2009) 192–198.
[25] C. Santoro, B. Li, P. Cristiani, G. Squadrito, Int. J. Hydrogen Energy 38 (1) (2013) 692–700.
[26] S. Brunauer, P.H. Emmett, E. Teller, J. Am. Chem. Soc. 60 (2) (1938) 309–319.
[27] C. Santoro, Y. Lei, B. Li, P. Cristiani, Biochem. Eng. J. 62 (2012) 8–16.
[28] X. Wang, C. Santoro, P. Cristiani, G. Squadrito, Y. Lei, A.G. Agrios, U. Pasaogullari, B. Li, J. Electrochem. Soc. 160 (7) (2013) G117–G122.
[29] G.W. Luther III, B.T. Glazer, S. Ma, R.E. Trouwborst, T.S. Moore, E. Metzger, C. Kraiya, T.J. Waite, G. Druschel, B. Sundby, M. Taillefert, D.B. Nuzzio, T.M. Shank, B.L. Lewis, P.J. Brendel, Marine Chem. 108 (2008) 221.
[30] F. Harnisch, S. Wirth, U. Schroder, Electrochem. Commun. 11 (11) (2009) 2253–2256.
[31] C. Santoro, M. Cremins, U. Pasaogullari, M. Guilizzoni, A. Casalegno, A. Mackay, B. Li, J. Electrochem. Soc. 160 (7) (2013) G128–G134.
[32] C. Santoro, I. Ieropoulos, J. Greenman, P. Cristiani, T. Vadas, A. Mackay, B. Li. Int. J. Hydrogen Energy. http://dx.doi.org/10.1016/j.ijhydene.2013.02.070.
[33] P. Cristiani, M.L. Carvalho, E. Guerrini, M. Daghio, C. Santoro, B. Li, Bioelectrochemistry 92 (2013) 6–13.
[34] F. Zhao, F. Harnisch, U. Schröder, F. Scholz, P. Bogdanoff, I. Herrmann, Environ. Sci. Technol. 17 (2006) 5193–5199.
[35] E. Guerrini, P. Cristiani, S. Trasatti, Int. J. Hydrogen Energy 38 (2013) 345–353.
[36] T.E. Fischer, S.R. Kelemen, J. Catal. 53 (1) (1978) 24–34.
[37] J.K. Dunleavy, Platinum Metals Rev. 50 (2) (2006) 110.
[38] G. Postole, A. Auroux, Int. J. Hydrogen Energy 36 (2011) 6817–6825.
[39] P. Ledezma, A. Stinchcombe, J. Greenman, I. Ieropoulos, Phys. Chem. Chem. Phys. 15 (7) (2013) 2278–2281.
[40] I. Ieropoulos, J. Greenman, C. Melhuish, I. Horsfield, Proceedings of the 12th International Conference on the Synthesis and Simulation of Living Systems, Odense. E-Book, ISBN: 10:0-262-29075-8 (2010), pp. 733–740.
[41] C. Melhuish, I. Ieropoulos, J. Greenman, I. Horsfield, Auton. Robots 21 (2006) 187–198.